Soft Matter

Cite this: *Soft Matter*, 2011, **7**, 6404

www.rsc.org/softmatter

COMMUNICATION

Biomimetic microlens array with antireflective "moth-eye" surface†

Doo-Hyun Ko,[a] John R. Tumbleston,[b] Kevin J. Henderson,[a] Larken E. Euliss,[c] Joseph M. DeSimone,[a] Rene Lopez[b] and Edward T. Samulski*[a]

Received 20th February 2011, Accepted 21st April 2011
DOI: 10.1039/c1sm05302g

We report a replication route to non-planar, three dimensional microlens arrays with an antireflective surface nanopattern. Our methodology uses the surface topography of the *Attacus atlas* moth's compound eye and a soft lithographic technique to fabricate topographically faithful moulds that, in turn, are used to reproducibly replicate the original eye surface with nanoscale fidelity. In addition to antireflection, the resulting poly(urethane) replica with its "moth-eye" nanopattern also exhibits increased hydrophobicity relative to the unpatterned polymer. The materials flexibility of the perfluoropolyether mould fabricated *via* replica moulding enables, for example, the embossing of antireflective nanopatterns in the photoactive materials of organic solar cells.

Photonic phenomena in biology have been refined by evolution and span diverse array of applications such as temperature control,[1] mate attraction,[2] antireflection,[3] and the efficient collection of low light levels.[4] And, biomimicry of natural visual systems has been exploited to enhance optical performance.[5–8] The *Attacus atlas* moth[9] is an insect that organizes its imaging system with a compound lens to accommodate its low brain processing capabilities.[10] The compound lens is characterized by a myriad of hexagonally shaped ommatidia each of which is an optical microlens that can produce an individual image thereby endowing a large field of view without an increase of the eye volume. Moreover, each ommatidium of the nocturnal moth has a unique nanometre scale surface structure—an antireflection (AR) nanostructure—which enhances photosensitivity in a dim environment concomitantly reducing reflections that could be visible to predators.[11,12] The sub-wavelength AR nanostructure on the moth ommatidial surface produces a gradual change in refractive index between the air and the eye interior, thereby reducing the reflection of incident light. Here we describe a method for direct and facile bio-replication of both micro- and nanoscale features of the *Attacus atlas* moth compound eye with a soft imprint lithographic method (replica moulding) that derives from a process called PRINT™ (Pattern Replication In Non-wetting Templates).[13]

3D Microlens arrays have a large field of view[10,14] hence, potential applications in wide angle imaging.[15] Currently, planar microlens arrays are fabricated with soft-lithography,[16] ink-jet printing,[17] an etched glass master,[18] 3D diffuser lithography,[19] thermal flow processing,[20] stimulus responsive hydrogels,[21] the hydrophobic effect,[22] three-beam interface lithography[23] and other advanced photolithographic methods. Polymerizing polydimethylsiloxane (PDMS) under humid conditions has also been used to fabricate such arrays,[24] and the artificial ommatidium fabricated with self-aligned waveguides[25] can potentially lead to truly biomimetic compound-eye sensors. Sub-wavelength, artificial AR moth eye surface patterns have been fabricated to improve optical performance using a variety of methods: colloidal crystal self-assembly,[26] colloidal lithography,[27–30] self-masked dry etching,[31] and imprinting,[32–34] for various optoelectronic devices[35–37] where the lowest reflectance and the highest transmittance are required. In summary, many attempts to combine the advantages of planar microlens arrays with AR properties have been explored.[38–40]

To date, however, only a limited number of curved 3D microlens arrays[14,25,41] have been reported because of complications associated with traditional fabrication methods. Addition of an AR surface nanostructure on a curved 3D microlens array further limits fabrication options. Herein, we replicate the ommatidial surface with its micro- and nanostructure to yield a 3D microlens array with AR properties. Our soft imprint lithographic method[13] is a replica moulding scheme employing an elastomeric perfluoropolyether (PFPE)[42] to fabricate multiscale surface features. PFPE proved to be advantageous relative to PDMS when replicating elaborate biological samples due to its low surface roughness, chemical inertness, polymerization characteristics, and its non-wetting, very low surface energy. We have captured the curved lens array of the *Attacus atlas* moth eye with its variable scale, hierarchical surface features in a PFPE mould that, in turn, was used to generate polymer replicas having all of the superficial features of that compound eye. Replicas made from UV curable polyurethane formulation (PU) act as 3D microlens arrays exhibiting AR properties as well as increased hydrophobicity.

The hierarchical structure of the *Attacus atlas* moth eye is shown in a sequence of SEM (scanning electron microscope) pictures at

[a]*Department of Chemistry, University of North Carolina at Chapel Hill, Caudill and Kenan Laboratories, CB 3290, Chapel Hill, NC, USA 27599-3290. E-mail: et@unc.edu*
[b]*Department of Physics and Astronomy, University of North Carolina at Chapel Hill, Phillips Hall CB 3255, Chapel Hill, NC, USA 27599-3255*
[c]*HRL Laboratories, LLC, Sensors and Materials Laboratory, 3011 Malibu Canyon Rd, Malibu, CA, 90265, USA*

† Electronic supplementary information (ESI) available: Description of fabrication details for PU and P3HT:PCBM moth eye replica, PDMS mould, optical properties of the used films and calculated reflection properties. See DOI: 10.1039/c1sm05302g

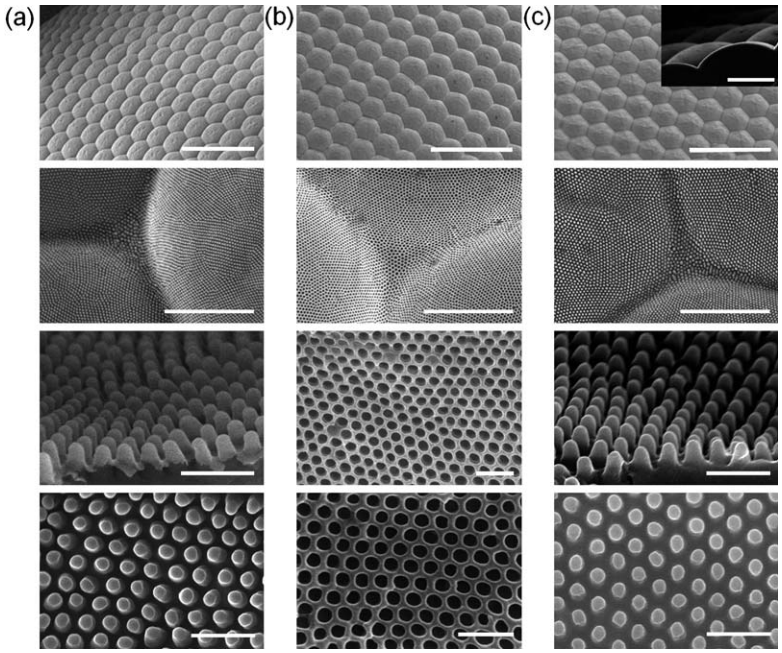

Fig. 1 SEM (Scanning Electron Micrographs) of (a) the *Attacus atlas* moth eye showing the compound eye structure; (b) the PFPE mould of the *Attacus atlas* moth eye; (c) a compound eye PU replica made by photopolymerizing the PU monomer in the PFPE mould. The inset of (c) shows the curved surfaces of the replica. The scale bars are respectively 100 μm for the top images (inset: 20 μm), 5 μm for the second row images, and 500 nm for the third and fourth row images.

different magnifications in Fig. 1: (a) the original moth eye, (b) the PFPE mould, and (c) the PU moth-eye replica. Fig. 1a shows that the moth eye is composed of an hexagonal array of the micrometre scale lenses. An AR nanopattern on the surface of each lens is apparent at increasing magnifications (top to bottom). A globally concave mould ("negative") comprised of the non-wetting PFPE is produced when the PFPE precursor in contact with the biological moth eye is photopolymerized (Fig. 1b; see Fig. S1 in the ESI† for detailed procedures). This unique elastic fluoropolymeric material not only reproduces the hemispherical global eye shape, but also captures the individuated convex lenses and delineates each lens's sub-200 nm features. A comparative study of the moulding properties of PFPE and PDMS to produce reusable concave microlens arrays was performed. (See Fig. S2 in the ESI†.) SEM analysis showed that the PDMS moulds exhibited excessive distortion and wrinkling, involved harsher conditions of polymerization, and PDMS replication has problems with liftoff which damaged the biological sample. These disadvantages are not encountered with PFPE.

The negative mould is used to produce a "positive" replica of the original eye topography from conventional photopolymer such as PU (Norland Products Inc., NOA 73) as shown in Fig. 1c. The fidelity of the fine structure of the moth eye is reproduced on a nanometer scale and the PU replica exhibits features identical to that of the original natural moth eye. The moth eye replica is ~4 mm diameter with a hemispherical global shape.

The compound eye of the moth produces an individual image of a projected object where the resolution of the image is restricted by the ommatidia number.[43] This is demonstrated for the moth eye replica when the symbol in Fig. 2a is projected into the microscope through the replica with the projected images captured by a camera. In Fig. 2b and c, each of the hexagonally arranged lenses in the moth eye replica generates an inverted image working as an individual lens. Interestingly the multiple images are produced by projecting a single object, and the size of the created images produced by the microlens replica is a function of the distance between the object and the replica. This might be exploited, for example, to generate multiple micropatterns on a photoresist coated surface.[44] It is known that moth eyes are superposition compound eyes and thus the images from each facet are not optically isolated producing superimposed images on the image plane (retina) and therefore yielding increased photosensitivity.[43] This originates from the fact that in the natural eye each optical element underneath each facet bends the incident light to form overlapping images on the retina. Here, the projected image is transmitted across a clear region underneath each lens facet, and the superposed images are focussed on a retina.[45] However, in our study only the exterior of each microlens is replicated resulting in multiple images by simple projection optics. Further optical manipulation of the projected images within the bulk of the replicated eye is required

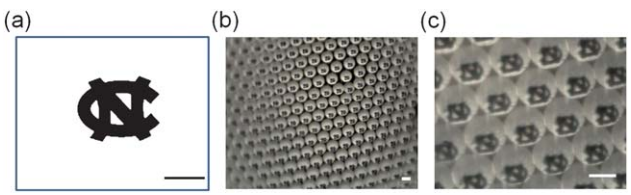

Fig. 2 Micrographs of multiple images generated by the moth eye replica. When the 2D symbol (3 mm length and 0.3 mm line width), printed on a transparent glass slide (a) is projected into the microscope through the moth eye replica (replicated 4 mm diameter PU microlens array), the multiple inverted images (b), shown at higher magnification in (c) are obtained by projecting the single object (a). The scale bars are 1.5 mm for (a) and 20 μm for (b) and (c).

to develop a single, superimposed image with enhanced intensity, a potentially useful goal for advanced optical devices.

Nocturnal survival probably dictated the evolution of the sophisticated structure of the moth eye.[12] The eye must effectively pass incident photons through the ommatidial surface while minimizing reflection. The latter is accomplished with a periodic array of subwavelength surface protrusions (Fig. 1a and 3c). The quasi-hexagonal nanopattern of protrusions with subwavelength periodicity causes a gradual transition between the air and the nanopatterned substrate resulting in low reflectance over a broad wavelength range in the visible.[46] This can be quantitatively analyzed by measuring reflection spectra for the natural moth eye and its replica relative to a flat polyurethane substrate. Such measurements were conducted with an optical microscope connected to a spectrometer using unpolarized white-light at normal incidence. Comparisons of the reflection from the replica and flat PU substrates in Fig. 3a show that the AR nanopattern significantly reduces reflection by as much as 5-fold. Remarkably, both the natural moth eye and its replica show less than 1% reflectivity in the visible region confirming the fidelity of the replicated AR nanopattern. The details of the latter are as follows: a quasihexagonal array of ~200 nm high parabolic protrusions of diameter ~100 nm (top) increasing to 170 nm (bottom), with a subwavelength periodicity of ~200 nm that is anticipated to exhibit significant broadband AR properties.[47] The observed AR trends can be checked by optical calculation (RSoft DiffractMOD) where a comparable nanopattern (155 nm height and 200 nm periodicity) is considered using the refractive indices of PU as measured *via* spectroscopic ellipsometry (see Fig. 3a, S3 and S4 in the ESI† for refractive indices of PU and reflection calculation details). In order to check the nanopatterns' contribution to the reduced reflection for the moth eye replica, we prepared a PU replica with the same global shape with a smooth surface (*i.e.*, we replicated a hemisphere from a ball bearing with curvature comparable to the moth eye) and measured the reflection (data are not shown) that was roughly equal to that of a flat PU film.

Besides improved AR properties, advantageous wetting characteristics are a by-product of the nanostructure. Fig. 4 shows contact angles assumed by water droplets on the PU moth eye replica. In order to remove the effects of macroscopic curvature on the apparent wetting properties, wetting of a comparable size (~4 mm diameter) PU sphere is also reported (Fig. 4b). A qualitative increase in the apparent contact angle[48] shows that the nanoscale protrusions on the moth-eye replica enhance hydrophobicity relative to the flat and spherical PU control substrates, advantageous for self-cleaning microlens arrays.[49] The mould is reusable. Fig. 4d and e show that identical nanopatterns created in the first and second replicas, *i.e.*, the soft imprint lithographic method with PFPE enables facile fabrication of multiple replicas.

Lastly, in an effort to emphasize the optical advantages of moth eye AR nanopatterns in general, it has been recognized that applying a superficial synthetic AR-coating on the surface of organic photovoltaic cells yields improved performance.[35] In this spirit, we embossed a microlens array with its AR surface nanopattern in the most widely used photoactive polymer for organic photovoltaic cells: a 1 : 0.8 blend of P3HT (poly(3-hexylthiophene) : PCBM(phenyl-C61-butyric acid methyl ester) (Fig. 5; see also the ESI† (Fig. S5) for the replication procedure details). Ongoing research[50] is exploring. such device applications, however the feasibility of using soft imprint lithography to emboss nanopatterns in photoactive material is apparent.

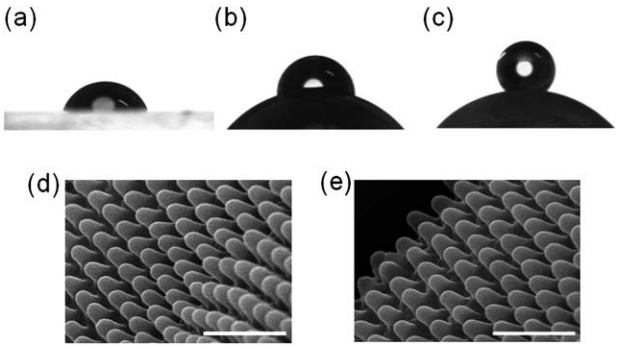

Fig. 4 Images of a water droplet on (a) a flat PU substrate, (b) a PU smooth sphere, and (c) the PU moth eye replica. Enhanced hydrophobicity of the PU replica with the moth eye AR nanopattern is apparent. The same PFPE mould used for the moth eye replica (d) is re-used to generate (e); identical dimension and feature shapes are derived from the second use of the PFPE mould. Scale bars in (d) and (e) are 500 nm.

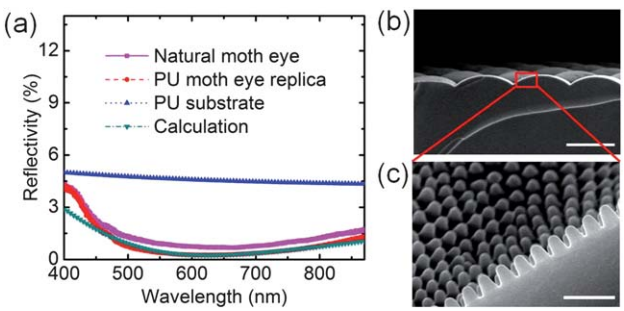

Fig. 3 Moth eye reflectivity and hierarchical surface structure. (a) Measured reflectivity for unpolarized light at normal incidence for a natural moth eye, its replica, a flat PU substrate, and an optical calculation. (b and c) SEM images of the replica. The parabolic protrusions result in broadband, anti-reflection. The scale bars are, respectively, 30 μm for (b) and 500 nm for (c).

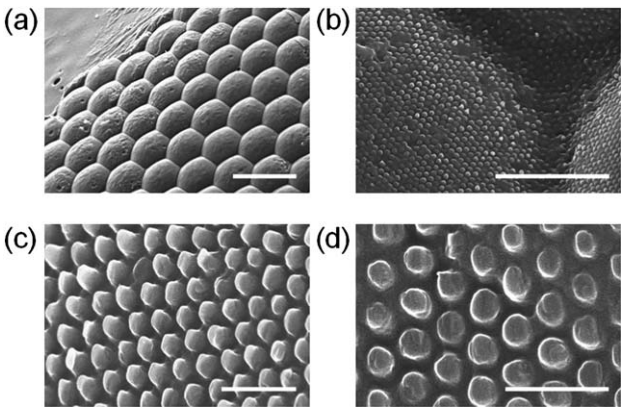

Fig. 5 SEM images of embossed P3HT:PCBM. (a) The compound eye shaped facets are replicated using the PFPE mould of the *Attacus atlas* moth eye; magnified SEM images of the patterned PV-active blend of P3HT:PCBM (b–d). Scale bars are (a) 50 μm, (b) 3 μm, (c) 500 nm and (d) 500 nm, respectively.

In conclusion, we have demonstrated a general way to simply fabricate 3D microlens arrays using naturally occurring biological structures. The fidelity of a replicated natural insect eye in conjunction with the range of materials compatible with the PFPE replica mould enables one to tailor microlens arrays of variable materials, sizes, shapes, and curvatures through this simple extension of biomimicry. The combined advantages of anti-reflectivity with hydrophobicity afforded by the multiscale micro- and nanopatterns are apparent. Compared to other methods of fabricating curved microlens arrays, we find this replication technique to be very easy, reproducible, and cost effective. The advantages of nonplanar compound microlens arrays produced with this methodology could be readily integrated into photovoltaics, optical sensors and optoelectronic devices.

Acknowledgements

Support for this work is from NSF (Solar: DMR-0934433), and D.H. K. thanks the UNC-Chapel Hill Institute for the Environment (Carolina Energy Fellows Program). K.J.H. acknowledges a Kauffman Fellowship and the UNC Office of Undergraduate Research. The American Chemical Society Petroleum Research Fund (no. 49187-DNI10) also partially supported this research. We thank Dr Amar Kumbhar for help with AFM (CHANL, UNC-Chapel Hill) and Dr Carrie Donley, Wallace Ambrose, Dr Robert Geil for stimulating conversations. We thank the Durham Museum of Life & Science for providing the moth specimen for this research.

Notes and references

1 L. P. Biró, Z. Bálint, K. Kertész, Z. Vértesy, G. I. Márk, Z. E. Horváth, J. Balázs, D. Méhn, I. Kiricsi, V. Lousse and J.-P. Vigneron, *Phys. Rev. E: Stat., Nonlinear, Soft Matter Phys.*, 2003, **67**, 021907.
2 R. L. Rutowski, *Anim. Behav.*, 1982, **30**, 108–112.
3 A. R. Parker and H. E. Townley, *Nat. Nanotechnol.*, 2007, **2**, 347–353.
4 J. Aizenberg and G. Hendler, *J. Mater. Chem.*, 2004, **14**, 2066–2072.
5 L. P. Lee and R. Szema, *Science*, 2005, **310**, 1148–1150.
6 J. Huang, X. Wang and Z. L. Wang, *Nano Lett.*, 2006, **6**, 2325–2331.
7 R. J. Martín-Palma, C. G. Pantano and A. Lakhtakia, *Nanotechnology*, 2008, **19**, 355704–355708.
8 R. J. Martin-Palma, C. G. Pantano and A. Lakhtakia, *Appl. Phys. Lett.*, 2008, **93**, 083901–083903.
9 S. Dey and B. Dkhar, *Micron Microsc. Acta*, 1992, **23**, 337–339.
10 J. W. Duparré and F. C. Wippermann, *Bioinspir. Biomimetics*, 2006, **1**, R1–R16.
11 D. G. Stavenga, S. Foletti, G. Palasantzas and K. Arikawa, *Proc. R. Soc. London, Ser. B*, 2006, **273**, 661–667.
12 C. G. Bernhard, *Endeavour*, 1967, **26**, 79–84.
13 J. P. Rolland, E. C. Hagberg, G. M. Denison, K. R. Carter and J. M. D. Simone, *Angew. Chem., Int. Ed.*, 2004, **43**, 5796–5799.
14 D. Zhu, C. Li, X. Zeng and H. Jiang, *Appl. Phys. Lett.*, 2010, **96**, 081111–081113.
15 Y. Kim, J.-H. Park, S.-W. Min, S. Jung, H. Choi and B. Lee, *Appl. Opt.*, 2005, **44**, 546–552.
16 M. V. Kunnavakkam, F. M. Houlihan, M. Schlax, J. A. Liddle, P. Kolodner, O. Nalamasu and J. A. Rogers, *Appl. Phys. Lett.*, 2003, **82**, 1152–1154.
17 S. Biehl, R. Danzebrink, P. Oliveira and M. A. Aegerter, *J. Sol-Gel Sci. Technol.*, 1998, **13**, 177–182.
18 P. Zhang, G. Londe, J. Sung, E. Johnson, M. Lee and H. Cho, *Microsyst. Technol.*, 2007, **13**, 339–342.
19 S.-I. Chang and J.-B. Yoon, *Opt. Express*, 2004, **12**, 6366–6371.
20 Y. Hsiharng, C.-K. Chao, M.-K. Wei and C.-P. Lin, *J. Micromech. Microeng.*, 2004, **14**, 1197–1204.
21 L. Dong, A. K. Agarwal, D. J. Beebe and H. Jiang, *Nature*, 2006, **442**, 551–554.
22 D. M. Hartmann, O. Kibar and S. C. Esener, *Opt. Lett.*, 2000, **25**, 975–977.
23 S. Yang, G. Chen, M. Megens, C. K. Ullal, Y. J. Han, R. Rapaport, E. L. Thomas and J. Aizenberg, *Adv. Mater.*, 2005, **17**, 435–438.
24 H. Yabu and M. Shimomura, *Langmuir*, 2005, **21**, 1709–1711.
25 K.-H. Jeong, J. Kim and L. P. Lee, *Science*, 2006, **312**, 557–561.
26 N. C. Linn, C.-H. Sun, P. Jiang and B. Jiang, *Appl. Phys. Lett.*, 2007, **91**, 101108–101103.
27 Y. Li, J. Zhang and B. Yang, *Nano Today*, 2010, **5**, 117–127.
28 J. Zhu, Z. Yu, G. F. Burkhard, C.-M. Hsu, S. T. Connor, Y. Xu, Q. Wang, M. McGehee, S. Fan and Y. Cui, *Nano Lett.*, 2009, **9**, 279–282.
29 Y. Li, J. Zhang, S. Zhu, H. Dong, F. Jia, Z. Wang, Z. Sun, L. Zhang, Y. Li, H. Li, W. Xu and B. Yang, *Adv. Mater.*, 2009, **21**, 4731–4734.
30 W.-L. Min, B. Jiang and P. Jiang, *Adv. Mater.*, 2008, **20**, 3914–3918.
31 Y.-F. Huang, S. Chattopadhyay, Y.-J. Jen, C.-Y. Peng, T.-A. Liu, Y.-K. Hsu, C.-L. Pan, H.-C. Lo, C.-H. Hsu, Y.-H. Chang, C.-S. Lee, K.-H. Chen and L.-C. Chen, *Nat. Nanotechnol.*, 2007, **2**, 770–774.
32 Q. Chen, G. Hubbard, P. A. Shields, C. Liu, D. W. E. Allsopp, W. N. Wang and S. Abbott, *Appl. Phys. Lett.*, 2009, **94**, 263118–263113.
33 S. Endoh and K. Hayashibe, *Jpn. J. Appl. Phys.*, 2009, **48**, 06FD04.
34 E.-J. Hong, K.-J. Byeon, H. Park, J. Hwang, H. Lee, K. Choi and G. Y. Jung, *Mater. Sci. Eng., B*, 2009, **163**, 170–173.
35 K. Forberich, G. Dennler, M. C. Scharber, K. Hingerl, T. Fromherz and C. J. Brabec, *Thin Solid Films*, 2008, **516**, 7167–7170.
36 H. Kasugai, Y. Miyake, A. Honshio, S. Mishima, T. Kawashima, K. Iida, M. Iwaya, S. Kamiyama, H. Amano, I. Akasaki, H. Kinoshita and H. Shiomi, *Jpn. J. Appl. Phys.*, 2005, **44**, 7414–7417.
37 J. Zhu, C.-M. Hsu, Z. Yu, S. Fan and Y. Cui, *Nano Lett.*, 2010, **10**, 1979–1984.
38 J.-T. Wu, W.-Y. Chang and S.-Y. Yang, *J. Micromech. Microeng.*, 2010, **20**, 075023–075026.
39 S. S. Oh, C.-G. Choi and Y.-S. Kim, *Microelectron. Eng.*, 2010, **87**, 2328–2331.
40 T. Yanagishita, K. Nishio and H. Masuda, *Appl. Phys. Express*, 2009, **2**, 022001–022003.
41 D. Radtke, J. Duparré, U. D. Zeitner and A. Tünnermann, *Opt. Express*, 2007, **15**, 3067–3077.
42 G. Sandra, M. Diez, A. Offenhäusser, M. C. Lensen and D. Mayer, *Nanotechnology*, 2010, **21**, 245307–245313.
43 K. Moses, *Nature*, 2006, **443**, 638–639.
44 L. Li and A. Y. Yi, *J. Micromech. Microeng.*, 2009, **19**, 105010–105018.
45 M. F. Land, *Pure Appl. Opt.*, 1997, **6**, 599–602.
46 S. J. Wilson and M. C. Hutley, *Opt. Acta*, 1982, **29**, 993–1009.
47 Y. M. Song, S. J. Jang, J. S. Yu and Y. T. Lee, *Small*, 2010, **6**, 984–987.
48 E. Bormashenko, *J. Phys. Chem. C*, 2009, **113**, 17275–17277.
49 C. Neinhuis and W. Barthlott, *Ann. Bot.*, 1997, **79**, 667–677.
50 D.-H. Ko, J. R. Tumbleston, W. Schenck, R. Lopez and E. T. Samulski, *J. Phys. Chem. C*, 2011, **115**, 4247–4254.